INFLUENCE OF PARAMETERS OF THE GLOW DISCHARGE ON CHANGE OF STRUCTURE AND THE ISOTOPE COMPOSITION OF THE CATHODE MATERIALS

I.B. SAVVATIMOVA AND D.V. GAVRITENKOV

FSUE, "RI SIA Luch", Moscow, Russia

Results of examinations of changes in structure, element, and isotope composition of cathodes after the glow discharge exposure in hydrogen, deuterium, argon, and xenon are submitted. The voltage of the discharge was less than 1000 V and the current was 5–150 mA. Samples before and after ions bombardment in the glow discharge were explored by the methods of mass spectrometry: the secondary ions (SIMS), the secondary ions with additional ionization of neutral sprayed particles (SNMS), spark (SMS), and thermo-ionization (TIMS), and also methods of energy dispersion X-ray spectral analysis (EDX). The alpha-, beta-, gamma- emission, and gamma- spectrometry for radioactive uranium specimens were also carried out before and after experiments in the glow discharge. Changes in structure, isotope, and element composition of the cathode samples depend on current density, integrated ions flow (fluence of ions), kind of irradiating ions and other experimental conditions. Attempts are made to estimate qualitatively and quantitatively the role of each of the parameters on intensity of the observed changes in cathode composition. It is shown that the maximum changes in structure, chemical and isotope composition of the cathode material occur in "hot points," such as craters from microexplosions, phase segregations, blisters and other new formations. Various methods of the analysis revealed that the basic elements Mg, O, Si, Al, and Ca with quantities up to per cents and more were prevailing in these zones and not found out before experiment. The greatest changes of the isotope relations were observed for iron, calcium, silicon, chromium after experiments with pulsing current. EDX method finds out the elements missing in the samples before experiment such as cadmium, strontium, tin. The isotopes with mass number 59 (Co 100%), 55 (Mn 100%), 45 (Sc 100%) are also not found in initial samples and background measurement by TIMS method. Results of changes in the element and isotope composition, which are found by various methods of the analysis, are compared with possible reactions of fusion-fission. It is noted that under different experimental conditions on various cathode materials similar groups of prevailing elements are find by various methods of the analysis.

1. Introduction

As is known, the ionic processing of materials results in changing surface properties. It has been shown earlier that physical–mechanical properties, element, and isotope compositions in plasma of a glow discharge change.[1−9]

The majority of the "additional" elements found after ion irradiation and not found before irradiation is distributed at the boundaries of grains[1] and in local spots.[3,4,9] They make up from the 10th fractions of a percent up to several

percents. Thus in initial samples the content of separate impurity elements did not exceed 10^{-3}–10^{-4} at.% and EDX analysis could not reveal it. Groups of such elements as Sc, Ti, V, Ag, Cd, In, P, Cl, Br, Ge, As, Kr, Sr, Y, Ru, and Xe have been found in Pd after irradiation by ions of all the types (D, H, Ar, and Ar+Xe), but in various quantities.[2] Elements with atom numbers $Z = 26$–31 (Fe, Cu, Zn, and Ga) were observed by the method of energy-dispersion X-ray spectral analysis (EDX) preferentially after irradiation by deuterium ions.

As a result of EDX and radiography, it was supposed that nuclear transmutations occur more intensively on local sites.[1–4] Distinctions in the characteristic spectrums corresponding to various combinations confirmed the nuclear processes in local zones.[3,9] Considerable changes of the isotope relations were observed for ^{10}B/^{11}B, ^{12}C/^{13}C, ^{60}Ni/^{61}Ni/^{62}, ^{40}Ca/^{44}Ca, and ^{90}Zr/^{91}Zr.[3] Change of the isotope relation in $^{109/107}$Ag from 3/1 up to 9/1 was observed in different series of experiments.[3,9]

In this paper, the changes of structure, element, and isotope composition of palladium for various parameters of the discharge are compared. The role of the current sort in transmutation intensity is shown. The possible types of nuclear reactions for pairs of the elements observed in the cathodes after experiments are shown.

2. Methods of the Analysis and Parameters of Glow Discharge

The installation had a vacuum discharge chamber with a cathode and an anode. The chamber was evacuated up to 10^{-2} Torr, and then it was filled by working gas up to 3–10 Torr. Deuterium, hydrogen, argon, and xenon were used as working gases. Samples were irradiated by currents with density of $\sim$10–50 mA/cm^2 and at discharge voltage of 50–1200 V. The discharge burning exposure was 1–40 h, diameter of samples $\sim$20 mm, thickness $\sim$100 μm, the irradiated area - about 1 cm^2. Multilayer cathodes consisting of several foils approximately 100 μm thick each for acquisition of data on change of the element and isotope composition on depth were used. The examinations procedure in detail is described in Refs. 3 and 9. The measurement system allowed recording current, discharge voltage, gas pressure, sample temperature, temperature of the inlet, output of the cooling water in the cathode, anode, and cooling jacket.

Changes in the element and isotope composition were analyzed by EDX methods and mass spectrometry. The element composition of the cathode materials was studied on scanning electronic microscope Hitachi S-840 with Link Analytical LS - 5 for a spectral analysis, later the structure of the surface and the sample composition were studied by electronic microscope JEOL JSM 6460-LV using INCA for X-ray spectral analysis. The content of elements was estimated using programs INCA (Version 4.02). Time of the spectra recording is 2 min. The accelerating voltage of 10 kV for the analysis of lighter elements and 30 kV for heavier elements were used. The analyzed zone size was about 1 μk^2 for the probe analysis in point, and when scanning on the area it was up to $\sim$250 $\times$ 200 μk^2. Sensitivity of the method was $\sim 10^{-2}$ atom.%. Depth of an analyzed layer made up about 1mk. Elements

O, F, S, Na, Mg, Al, Ti, Cr, and Fe are analyzed on Kα, Mo and Br - on Lα, W - on Mα of characteristic spectrums lines. Concentration of forming ("additional") impurity elements was determined given of the majority of lines of series in characteristic spectrum.

Initial samples and samples after experiments in deuterium glow discharge are analyzed. Places with structural defects and new formations such as swellings (blisters), craters, areas of micromeltings, needle structures, and sites of surface without special changes after irradiation in glow discharge plasma were explored.

The isotope composition of the samples at high temperature was determined by the method of the thermo-ionization mass spectrometry on mass spectrometer "Finnigan"-262. The sample temperature in this analysis usually exceeded 1800°C. The majority of complex compounds should break up (dissociate) at such a temperature while the secondary ionic mass spectrometry can give many composite complexes.

3. Changes in Structure of Surface, Element, and Isotope Composition

It is shown that changes of structure, element, and isotope composition depend on the following:

(a) Doses of irradiating ions (Tables 1–3).[1]
(b) Density of ions current (Tables 4 and 5).[3,4]
(c) Irradiating ions kind (Tables 4 and 5).[3–5]
(d) Current sorts: direct or pulsing (Tables 6, 12, and 13).
(e) Places of "hot points" analysis and new formation (Tables 8–12).

Each of the above process parameters (a–d) influenced on the process intensity and its reproducibility. The role of "hot points" in the change of structure, chemical, and isotope composition[3–5] and the groups of the elements dominating in these "active sites" are analyzed by various methods.[1,2,5] In this paper special attention is paid to structural change in new formations (in zones of craters, growth formations, and blisters) and to the effect of current (direct and pulsing).

3.1. *Dependence of "Additional" Elements Quantity on Dose*

Changes of the isotope and element composition of the samples irradiated by deuterium ions after different exposure time (dose) were analyzed by several methods. Table 1 comprised the data received by method of secondary ionic mass spectrometry after 30 min bombarding of palladium by deuterium. Table 2 includes the results of EDX data, and Table 3 has the same samples data obtained by method of spark mass spectrometry.

The increase in the content of Li by a factor of 50–450 (rows 1 and 2), ^{11}B by a factor of 70 (row 4) can be a result of nuclear process under conditions of low-energy actions in glow discharge plasma with the participation, for example, of hydrogen

or deuterium, or processes of heavier elements fission. The increase in the content of Zr by a factor of ∼340 (rows 15 and 16), V by a factor of 100 (row 5), Cr by a factor of 160 (row 6), Fe by a factor of 2 (rows 9), and Ni - 5–30 (rows 10 and 11) can also be a result of nuclear transmutations. The experimental time of this series was ∼30 min. The increase of the impurity elements at the backside was observed only for Li. "Dot" aggregations of Zn, Co, Br, and Mg located preferentially on boundaries of subgrains, with a density of $\sim(1–10)\times10^6$ cm^{-2} (for Zn the density of such places made up $\sim(1–2)\times10^6$ cm^{-2}, for Br$\sim(2–4)\times10^6$ cm^{-2})[1] are found during scanning the surface of a sample.

Table 1. Changes of isotope and element composition of impurity atoms on surface of palladium after bombarding by deuterium ions (SIMS).[3]

No.	Mass number	Element	Content (arb.un.)		
			Before experiment	After experiment	
				Irradiated side	Back side
1	6	Li*	0.02	1.00	0.15
2	7	Li*	0.02	9.00	0.28
3	10	B*	0.01	0.01	0.01
4	11	B*	0.10	7.00	0.01
5	51	V*	0.30	30.00	0.20
6	53	Cr	0.60	96.00	1.00
7	54	Fe, Cr	2.20	15.00	2.00
8	56	Fe	22.20	55.00	20.00
9	57	Fe	11.00	45.00	12.00
10	60	Ni	0.10	3.00	0.20
11	61	Ni	0.20	10.00	0.20
12	63	Cu	1.40	60.00	1.00
13	87	Sr*	0.10	1.00	0.10
14	88	Sr*	0.50	0.10	0.20
15	90	Zr*	0.00	57.00	0.00
16	91	Zr*	0.10	34.00	0.10

Thickness of the samples ∼ 100 μm. Depth of analyzed layer was ∼ 100 Å.
Method of the analysis secondary ionic mass spectrometry.
Li, B, V, Sr, and Zr were not present at the discharge chamber earlier.
The source of possible impurity is absent.

The comparison of the new elements quantity shows that an increase in experimental time (fluence) by a factor of 10 times (data EDX) leads only to an increase in Mo which is an element of construction (the a pressure holder of the sample, screening a part of surface during sample irradiation). Therefore, it is not surprising that irradiation time increase leads to Mo quantity increase. The quantity of other "additional" elements (Br, Sr, and Te which are absent in the sample before experiment) does not change largely with an increase of experimental time (a dose of irradiation) by a factor of 10.

The reason for such an effect can be both preferred formation of these elements in the sample at the initial stage of the discharge burning, having significant quantity of

different defects on its surface and possible preferable sputtering of lighter elements at the following experimental stage. Another reason for the absence of growth of the "additional" elements quantity with an increase in discharge burning time can be participation of the forming elements in the secondary reactions. It is impossible to exclude the contribution of irradiated surface screening by sputtered. However, the analysis of the same samples by spark mass spectrometry method does not confirm the explanation of the results obtained by the surface screening by molybdenum precipitation because an increase of other elements such as ^{7}Li, ^{11}B, K, Rb, In, and Nb in a longer experiment was observed both on irradiated and on the backside of the same sample.

Table 2. Additional atoms on palladium surface after glow discharge in deuterium (EDX).[1]

No.	The additional atoms	The nuclear number	Dependence of quantity of impurities on duration of experiment ($\times 10^{-2}$ at. %)	
		4 h	40 h	
1	Na	11	7.0 ± 0.3	3.0 ± 0.3
2	Mg	12	1.0 ± 0.3	2.0 ± 0.3
3	Al	13	4.0 ± 0.3	2.0 ± 0.3
4	Si**	14	1.5 ± 0.3	< 0.3
5	Ca	20	4.0 ± 0.3	3.0 ± 0.3
6	Ti*	22	1.0 ± 0.3	1.5 ± 0.3
7	Br*	35	3.0 ± 0.6	2.0 ± 0.6
8	Sr*	38	7.0 ± 0.6	6.0 ± 0.6
9	Y*	39	40.0 ± 1.0	20.0 ± 1.0
10	Mo**	42	15.0 ± 1.0	40.0 ± 1.0
11	Tc*	43	20.0 ± 1.0	10.0 ± 1.0

*Source of possible pollution is absent.
**Source of possible pollution is the parts of the construction.
Sonde diameter was 1 μm.
EDX method used SEM "HITACHI-800" with "Link Analytical" device.
All the peaks corresponding to Ti, Br, Sr, Y, and Tc on X-ray spectrums were observed after experiments.
Ti, Br, Sr, Y, and Tc were never present in the discharge chamber before experiment. Ti, Br, Sr, Y, Tc, Zn, and Co are absent before experiments in spectrums of this Pd.

A 500–3000-fold increase in Zr content (rows 20 and 21) can be a result of possible nuclear processes under low-energy actions in glow discharge plasma. One can assume that a 10–20-fold increase in Indium content (series 28) can also be an effect of stimulated nuclear processes with the participation of palladium and, for example, hydrogen, deuterium, or boron (mass numbers 10, 11). The assumption of preferred sputtering of light elements forming during experiment can confirm the data of Table 3 obtained by SMS method. One can see an increase in ^{10}B content by a factor of 2 on the sample backside with 4-hour irradiation and an increase in ^{11}B by a factor of 10 on the sample backside after 40-h experiment, and only by a factor of $\sim$3 on the irradiated side of samples (40 h). Increasing Al, ^{115}In, and

^{93}Nb correlate with an increase of the discharge time both on the irradiated and on backside of the sample. Similar changes are also observed for ^{90}Zr isotope on the surface irradiated by palladium ions where the increase is ∼500 times after 4-hour discharges and 1200 times for 40 h. On the backside, the quantity of ^{90}Zr increases by a factor of ∼4.4. The quantity of ^{91}Zr isotope increases ∼1000 and ∼1200 times with a 10-fold increase in discharge time. The ^{80}Se increasing was ∼100 times on

Table 3. Quantity of the impurity atoms on palladium surface after deuterium ions irradiation at glow discharge (SMS).[1]

No.	Mass number	Element	Content before ($\times 10^{-4}$ at. %) ($\times$ 100 ppm)	Additional element content in Pd for different experiment duration ($\times$ 10^{-4}at. %)			
				4 h		40 h	
				Upper	Lower	Upper	Lower
1	6	Li	0.06	0.15			
2	7	Li	0.06	0.33	0.40	0.90	0.50
3	10	B	0.07		0.15		
4	11	B	0.07	0.30	0.20	0.20	0.70
5	23	Na	0.44	4.40	1.00	2.00	6.00
6	27	Al	6.00	96.00	10.00	300.00	25.00
7	28	Si**	9.00	18.00	9.00		3.00
8	29	Si**	7.00	21.00	11.00		10.00
9	30	Si**	6.00	18.00	4.50	15.00	66.00
10	32	S	7.00	14.00	2.00	3.50	2.00
11	39	K	3.00	9.00		12.00	4.50
12	41	K	3.00	12.00	1.00	18.00	9.00
13	47	Ti*	1.20	1.80	60.00		
14	48	Ti*	1.40	580.00	2.50		3.50
15	49	Ti*	1.30	680.00	3.25	130.00	2.60
16	50	Ti*	1.70		3.40	130.00	
17	78	Se*	0.23	0.23	0.20	0.20	4.00
18	80	Se*	0.30	0.20	0.20	0.20	33.00
19	85	Rb*	< 0.03	0.01	0.05	90.00	51.00
20	90	Zr*	< 0.05	25.00	0.05	60.00	0.22
21	91	Zr*	< 0.05	50.00	0.05	61.00	
22	93	Nb*	< 2.00	40.00	2.00	7200.00	4.00
23	98	Mo**	0.40				3.00
24	100	Mo**	1.80	4500.00	1.80	2880.00	
25	103	Rh*	7.00	21.00	21.00	25.00	7.00
26	107	Ag*	1.00	63.00	3.00	1.00	3.20
27	109	Ag*	1.00	50.00	1.50		2.50
28	115	In*	< 0.04	0.48	0.04	0.80	0.16

*Possible source of impurity is absent.
**Possible source of Mo and Si impurities are construction parts.
Depth of analyzed layer $\sim 10\,\mu$m.
Sensitivity of the method 10^{-6}at. %.
The quantity of each isotope is brought to 100 %. Ti, Se, and Ru, In were not present before discharge experiments.
The sample irradiated by ions and contacting
"Lower" sample was not irradiated by deuterium ions and did not contact deuterium plasma.

backside for 40-hour experiment. Authors could not explain a significant increase in ^{11}B, ^{115}In, ^{93}Nb, ^{80}Se и ^{91}Zr on the backside of the sample by other non-nuclear processes.

3.2. *Dependence of Quantity of "Additional" Elements on Current Density and Ions Kind*

Current density (ions flow) and ions type are also important parameters the quantity of the impurity elements in the cathode material after discharge experiments depends on them. The data of other series experiments for quantities of Ag in Pd at various density of ions flow with different ion content are shown in Tables 4 and 6.

Table 4. Change of quantity of Ag in Pd glow-discharge cathode (SMS)[4].

Sample number	Current (mA)	Ions type	Analyze place*	Ag^{+2} (ppm)		Increasing (times)
				Isotope mass		
				107	109	
Initial	0		1	1.7×10^1	2.2×10^1	
			1	$\underline{5.0} \times 10^3$	$\underline{5.2} \times 10^3$	$\sim 2.5 \times 10^2$
1666	35	D_2	2	$\underline{2.1} \times 10^3$	$\underline{2.2} \times 10^3$	$\sim 1.0 \times 10^2$
			3	$< 1.5 \times 10^1$	< 5	–
			1	1.1×10^2	7.7×10^1	~ 4.0
1667**	35	H_2	2	$< 2.0 \times 10^1$	$< 2.0 \times 10^1$	–
			3	$< 2.0 \times 10^1$	$< 2.0 \times 10^1$	–
			1	$\underline{5.7} \times 10^2$	$\underline{5.6} \times 10^2$	$\sim 2.5 \times 10^1$
1668	25	H_2D_2	2	$\underline{6.9} \times 10^2$	$\underline{7.4} \times 10^2$	$\sim 3.5 \times 10^1$
			3	1.2×10^2	1.3×10^2	~ 5.0
1670	25	H_2	1	$\underline{9.7} \times 10^2$	$\underline{1.0} \times 10^3$	$\sim 5.0 \times 10^1$
			2	4.5×10^2	4.5×10^2	$\sim 2.0 \times 10^1$
1671	25	D_2	1	$\underline{2.6} \times 10^3$	$\underline{2.7} \times 10^3$	$\sim 1.2 \times 10^2$
			2	1.8×10^2	1.9×10^2	~ 9.0

$*1, 2, 3$ depth of analyzed layer is $10\,\mu$m: (1, 2) the upper irradiated sample; (3) unirradiated lower sample.
** 1668 - discharge in hydrogen, and then in deuterium.
ppm: impurities particles per million.

One can see that the maximal Ag increase after deuterium discharge at greater density of current (35 MA) in the near-surface layer of $10\,\mu$m was 250 times (from 20 ppm in an initial state up to 5000 ppm after irradiation by deuterium). The following layer $\sim 10\,\mu$m thick only showed $\sim$a 100-fold Ag increase. A lower increase ($\sim$120 times) of Ag content was observed at smaller current density (25 MA). A less increase was observed in hydrogen at greater current density.

It can be explained by easier output of hydrogen implanted into palladium lattice at a higher temperature of the sample (and accordingly by a smaller hydrogen content in palladium lattice), i.e. by closely related velocities of hydrogen implantation

and hydrogen desorption under these conditions. An essential increase of Ag content in the lower sample (∼4 times) was observed only for the sample preliminarily irradiated by hydrogen and then by deuterium. This might be a result of simultaneous running of both non-nuclear (sputtering, diffusion separation) and nuclear processes (fusion and fission, secondary interaction of nuclear reactions products).

Table 5 shows experimental data on B, Ni, and Zr. An increase of boron, nickel and zirconium isotopes was observed only at irradiation by deuterium and preferentially in the near-surface layer.

Table 5. Change of In, Ni, and Zr quantity in Pd cathode at deuterium discharge (SMS).

Sample number	Current (mA)	Gas	Analyzed layer	Isotope ($\times 10^{-4}$ at. % (ppm))							
				B		Ni				Zr	
				10*	11	58	60	61	62	90	91
Initial	0		1	<2.7	<0.4	10	<5.5	<40	<14	<1	5
			1	21	19	280	300	480	500	25	16
1666	35	D_2	2	<2	<2.5	60	69	<52	75	8,5	5
			3	<2.8	<1, 8	26	17	<36	<15	<1	<2, 4
1671	25	D_2	1	25	22	190	180	560	660	30	31
			2	<1.5	1.1	31	28	<80	<25	0.9	<5

3.3. *Dependence of Change in Pd Composition on Current Type*

3.3.1. *Change of the isotope and element composition of Pd sample under direct current discharge (TIMS)*

Isotope and element composition change for two different Pd samples (Table 6) arranged one above the other are given as an example, and the difference in isotopes ratio in them is shown. Light elements remains in the lower sample screened from direct ions irradiation. So, Al was found to be 10 times more in lower sample, Mg was also observed to be 4 times more in the lower sample, 29 mass (Si) was observed in the lower sample too. But ^{22}Ne (9.25%) isotope was observed in the upper Pd foil while ^{20}Ne (90.48%) was practically never observed. The absence of the isotope with maximum abundance is observed for mass numbers 18 and 15 (^{18}O and ^{15}N, respectively).

The following features in the isotope composition of the upper sample irradiated and the lower sample screened were observed:

- Absence of isotopes correlation in Ca and Ti with the natural abundance.
- Sc in the irradiated sample - 1200 counts per second (cps) in the lower one - 95 (cps). Sc was not available in the initial sample and the background analysis.

Cr and Fe were not available in the discharge chamber parts (water-cooled stainless steel holder was placed under eight Pd foils 100 μm thick each and one molybdenum foil 0.1 mm thick). Cobalt and manganese have not also been found in initial Pd and in background measurement. Cr, Fe, Co, and Mn were observed in the second sample in smaller quantities. Therefore, Mn intensity in the upper sample was 4000 cps and only ∼30 cps in the lower Pd sample. Cobalt quantity was found to be ∼380 cps in the upper sample and 20 cps in the lower sample, ^{52}Cr was ∼10 000 and ∼3400 cps, respectively. Only ^{44}Ca, ^{24}Mg, and Al were found to be in bigger quantities in lower Pd sample as compared with the upper sample.

Table 6. Isotope and element composition of Pd samples irradiated by deuterium ions under direct current discharge (TIMS).

Mass	Element	Natural abundance (%)	N_1 CPS, 1610(1)	N_2 CPS, 1610(2)	Δ (N_2-N_1)
14	N	90.6	–	–	
15		0.37	2.0×10^1	–	-2.0×10^1
16	O	99.8	–	–	
18		0.20	1.0×10^1	–	
22	Ne	9.32	6.0×10^1	1.0×10^1	-1.0×10^1
24	Mg	78.99	1.0×10^1	3.8×10^1	$+2.8 \times 10^1$
25		10	–	1.0×10^1	$+1.0 \times 10^1$
26		11	–	–	
27	Al	100	1.0×10^3	1.0×10^4	$+9.0 \times 10^3$
28	Si	92.23	2.5×10^2	1.0×10^2	-2.4×10^2
29		4.68	–	$1,5 \times 10^2$	$+1.5 \times 10^2$
30		3.09	–	3.0×10^1	$+3.0 \times 10^1$
42	Ca	0.65	1.8×10^3	1.5×10^2	-1.65×10^3
43		0.14	4.3×10^3	$1,5 \times 10^2$	-4.15×10^3
44		2.09	1.0×10^1	6×10^2	$+5.9 \times 10^2$
45	Sc	100	1.2×10^3	9.5×10^1	-1.1×10^3
46	Ti	8.0	5.0×10^1	6.5×10^1	$+1.5 \times 10^1$
47		7.3	3.0×10^1	5.5×10^1	$+2.5 \times 10^1$
48		73.8	1.2×10^2	4.0×10^2	$+2.8 \times 10^2$
49		5.5	1.0×10^1	4.5×10^1	$+3.5 \times 10^1$
50	Ti, Cr	5.4; 4.3	4.6×10^2	2.0×10^2	-2.6×10^2
51	V	99.8	4.6×10^2	5.0×10^2	$+4.0 \times 10^2$
52	Cr	83.8	1.0×10^4	3.4×10^3	-6.6×10^3
53	Cr	9.5	7.0×10^2	3.0×10^2	-4.0×10^2
54	Fe,Cr	5.8; 2.37	2.0×10^3	$2,6 \times 10^2$	-1.7×10^3
55	Mn	100	4.0×10^3	3.0×10^1	-3.0×10^3
56	Fe	91.7	1.5×10^4	2.5×10^3	-1.2×10^4
57	Fe	2.2	1.5×10^3	5.5×10^1	-1.4×10^3
58	Fe	0.28	3.8×10^2	3.0×10^1	-3.5×10^2
59	Co	100	3.8×10^2	2.0×10^1	-3.6×10^2

1610(1)—irradiated sample (N_1); 1610 (2)—screened sample located under irradiated sample (N_2).

A change of the isotope ratio in samples after carrying out deuterium bombardment was observed from several percent up to hundreds.[1,2] The quantities of "additional" elements were from 0.1 at.% up to $\sim$ 5 at.%. The most considerable difference in the isotope ratio was observed for Mg, Si, K, S, Ca, and Fe isotopes after deuterium discharge.

A comparison of the chemical composition and isotope ratio on palladium samples after experiments in deuterium discharge with direct current and pulsing current by thermo-ionization mass spectrometry is shown in Tables 7–10.

One can see from Table 8 that the quantity of Mg (24–26) and Si (28–30) isotopes in the lower layers of the sample are higher; therefore it is impossible to explain this fact by "impurity" from the surface.

Table 7. Change of Fe, Cr, and Ti isotope ratio with direct current by TIMS (No. 1610).

Sample number*	Element	Isotopes	Natural abundance (N_n)	Ratio after experiment (Nexp)	K**
1	Fe	56/57	$91.72/2.2 = 41.7$	$1.5 \times 10^4/1.5 \times 10^3 = 10$	4.17
2				$2.5{\times}10^3/5.5{\times}10^1 = 46.4$	0.90
1	Cr	52/53	$83.8/9.25 = 8.8$	$1.0{\times}10^4/7.0{\times}10^2 = 14.3$	0.62
2				$3400/3.0 \times 10^2 = 11.3$	0.78
1	Ti	48/47	$73.8/7.3 = 10.12$	$1.2 \times 10^2/3.0 \times 10^1 = 4$	2.50
2				$4.0 \times 10^2/5.5 \times 10^1 = 7.3$	1.40
1	Ti	48/46	$73.8/8 = 9.82$	$1.2 \times 10^2/5.0 \times 10^1 = 2.4$	3.80
2				$4.0{\times}10^2/6.5{\times}10^1 = 6.15$	1.50
1	Ti	48/49	$73.8/13.42 = 13.42$	$1.2 \times 10^2/10^1 = 12$	1.10
2				$4.0 \times 10^2/4.5 \times 10^1 = 8.9$	1.50

*(1) An irradiated sample, (2) the sample located under irradiated one.
** $K = N_n/N$ exp: natural ratio/ratio after experiments.

3.3.2. *Change of isotope and element composition in palladium at deuterium discharge under pulsing current*

These results (Tables 9 and 10) apply to the experiments with pulsing current frequency of $\sim 1.35 \times 10^3$ Hz, pulse length duration of 70 μs and a weak magnetic (magnetic field was $\sim$ 4 T). Average current is $\sim$ 10–15 mA, current in an impulse is $\sim$ 100–150 mA. A very essential increase (1000 times) of the isotopes ratio in pulsing current experiments essentially for isotopes of iron takes place. The contribution of heavy isotopes for such elements as Ni ($\sim$ 11–16 times) and Cr ($\sim$ 8 times) also decreases. For Ti and Ba the contribution of a heavier isotope increases 2–3 times. It is important to note that changes in ratios of lead (1 ± 0.1) and gallium (1.5 ± 0.1) isotopes after the experiments are not practically observed.

Table 8. Change of Fe, Cr, and Ti isotope ratio with direct current by TIMS (No. 1694).

Mass number	Element	Natural abundance (%)	Before exp. (s^{-1}*)	After exper. (s^{-1})	Natural isotope ratio (N_n)	Isotopes ratio after exp. ($N_{exp.}$)	K	Δ (s^{-1})
1	2	3	4	5	6	7	8	9
24	Mg	78.99	0	$50/8 \times 10^2$	$24/25 \sim 8$	$24/25 \sim 12$	~ 0.7	$+8 \times 10^2$
25		10	0	0/67	$25/26 \sim 1$	$25/26 \sim 1/0.5$	~ 2	+67
26		11	0	0/38	$24/26 \sim 8$	$24/26 \sim 1/0.5$	~ 2	+38
28	Si	92.23	0	$1 \times 10^2 / > 1 \times 10^2$	$28/29 \sim 20$	$28/29 \sim 0.16$	1×10^2	$+1 \times 10^2$
29		4.67	0	$6.3 \times 10^2 / 1 \times 10^3$				$+1 \times 10^3$
30		3.1	0	$2.2 \times 10^2 / 5 \times 10^2$	$28/30 \sim 30$	$28/30 \sim 0.5$	~ 60	$+5 \times 10^2$
40	Ca	96.86		1×10^6	$40/44 \sim 50$	$40/44 \sim 5$	~ 10	
42		0.6	3×10^3	2×10^5	$44/42 \sim 3$	$44/42 \sim 2.5 \times 10^{-2}$	$1,2 \times 10^2$	$+1,97 \times 10^5$
43		0.15	2×10^2	$\sim 4 \times 10^3$	$44/42 \sim 13.3$	$44/42 \sim 1.25$	~ 10.6	$+3,8 \times 10^2$
44		2.0	1×10^3	$\sim 5 \times 10^3$				$+4 \times 10^3$
45	Sc	100	0	2×10^2				$+2 \times 10^2$
46	Ti	8	65	1.3×10^3	$48/46 \sim 6.2$	$48/46 \sim 5.46$	~ 1.14	+1235
47		7.3	95	0				−95
48		73.8	1×10^3	7×10^3				$+6 \times 10^3$
56	Fe	91.7	2800	4500	$56/57 \sim 41.7$	$56/57 \sim 18$	~ 2.3	$+1.8 \times 10^2$
57		2.2	50	2.5×10^2				$+2 \times 10^2$
59	Co	100	0	1.5×10^3				$+1.5 \times 10^3$

*cps: counts per second.
**Δ, cps: difference of counts per second.
K: factor of change in natural isotopes ratio to isotopes ratio after experiment (N_n/N_{exp}).
Column 5: data of the second scanning of the same sample are through dash.

Table 9. Change of isotope and element composition in palladium at deuterium discharge under pulsing current (TIMS, # 1799).

Element	Mass number	Natural abundance (%)	After experiment (cps)
Ne	20	90,5	2.0×10^1
	21	0,27	3.0×10^1
	22	9,32	5.0×10^1
Ni	58	68.1	1.5×10^2
	60	26.2	6.5×10^2
Ni	61	1.25	3.0×10^1
	62	3.6	1.3×10^2
Fe	56	91.7	1.6×10^2
	57	2.2	4.0×10^3
Cr	52	83.8	4.8×10^2
	53	9.5	4.5×10^2
Ti	48	73.8	2.0×10^2
	47	8	1.0×10^1
Ga	69	60	3.0×10^2
	71	40	1.8×10^2
Ba	138	71.7	3.0×10^3
	137	11.3	1.9×10^2
	136	7.85	1.2×10^2
	135	6.6	2.2×10^2
	134	2.4	2.5×10^2
Pb	206	23.6	4.0×10^1
	207	22.6	4.8×10^1
	208	52.3	1.0×10^2

3.4. *"Additional" Elements Quantity on Different Methods of Analysis*

One can see that most essential changes of the element composition in rather considerable areas of surfaces and in the local microzones characterized by some different structural changes (Table 11 with EDX data and Figs. 1–4) were observed. TIMS method can show very thin changes in the surface layers, but these measurements will concern all areas of the analysis.

If we carried out spark mass spectrometry analyses, we found considerably smaller quantities, about 10^{-4} nuclear percent. However, the analyzed layer depth was $\sim$10 μm. Therefore, the depth of X-ray spectral analysis is $\sim$10 times less, and the depth of TIMS analysis is $\sim$100 times less than for SMS. Taking into account the analysis depth of spark mass spectrometry and correlate it with TIMS data and (or) EDX method, it is possible to assume that TIMS data in the thin surface layer was also $\sim$ 0.1–0.6%. Thus, each method of the surface analysis is important and should be taken into account. Therefore, the analysis of the samples before and after experiments was carried out, at least, by two different methods (e.g., EDX and TIMS).

Table 10. Isotope ratio change in "additional" elements of Pd sample after pulsing current experiment.

Element	Isotopes	Natural isotopes ratio (N_n)	Ratio after experiment ($N_{\exp}$)	K^{**}
Si	28/29	$93.2/4.7 = 22.6$	$10/75 = 0.13$	1.7×10^2
	28/30	$93.2/3.1 = 29.8$	$10/20 = 0.5$	6.0×10^2
Ne	20/21	$90.5/0.27 = 33.5$	$20/30 = 0.67$	5.0×10^2
	20/22	$90.5/9.329.7$	$20/50 = 0.4$	2.4×10^2
Ni	58/60	$68.1/26.2 = 2.6$	$1.5 \times 10^2/6.5 \times 10^2 = 0.23$	1.1×10^1
	58/61	$68.1/1.25 = 55$	$1.5 \times 10^2/3 \times 10^1 = 5$	1.1×10^1
	58/62	$68.1/3.6 = 19$	$1.5 \times 10^2/1.3 \times 10^2 = 1.15$	1.6×10^1
Fe	56/57	$91.2/2.2 = 41.45$	$1.6 \times 10 \times /4 \times 10^3 = 0.04$	1.0×10^3
Cr	52/53	$83.8/9.5 = 8.82$	$4.8 \times 10^2/4.5 \times 10^2 = 1.066$	8.0×10^1
Ti	48/47	$73.8/8 = \sim 9$	$2 \times 10^2/10 = 20$	5.0×10^{-1}
Ba	138/137	$71.7/11.3 = 6.35$	$3 \times 10^3/1.9 \times 10^2 = 15.8$	4.0×10^{-1}
	138/136	$71.7/7.85 = 9.13$	$3 \times 10^3/120 = 25$	3.6×10^{-1}
	138/135	$71.7/6.6 = 10.8$	$3 \times 10^3/2.2 \times 10^2 = 13.63$	8.0×10^{-1}
	138/134	$71.7/2.4 = 29.8$	$3 \times 10^3/2.5 \times 10^2 = 12$	2.5×10^1
Pb	208/207	$52.3/22.6 = 2.31$	$1 \times 10^2/48 = 2.0$	1.1×10^1
	208/206	$52.3/23.6 = 2.22$	$1 \times 10^2/40 = 2.5$	9.0×10^{-1}

K^{**}: A factor of change in natural isotopes ratio to isotopes ratio after experiment ($N_n/N_{\exp}$).

The "geometric" factor shows the influence of boundary conditions (Fig. 3a and b). The maximal surface change was observed at the interfaces between radiated and unirradiated (screened) areas. The screened areas had the insignificant change in topological structure and chemical structure.

Table 11. Dependence main elements on palladium surface for various methods of analysis of the same sample.

Element	Atomic % (EDX)*	TIMS (cps)**
Mg	3.1 ± 0.2	–
Fe	6 ± 0.2	$\sim 5.0 \times 10^3 \pm 2.5 \times 10^2$
Al	3.7 ± 0.2	$\sim 9.0 \times 10^5 \pm 2.5 \times 10^3$
Ga	2.4 ± 0.4	$\sim 7.0 \times 10^3 \pm 2.5 \times 10^2$
O	50 ± 1.5	–
Ca	2.7 ± 0.3	$\sim 2.2 \times 10^3 \pm 1 \times 10^2$ (42, 43, 44 isotopes)
Ti	4.3 ± 0.3	–

* The volume of analysis by X-ray spectral method (EDX) on electronic microscope JEOL JSM $\sim 1\,\mu m^3$.
** TIMS: thermo-ionization method; cps: impulses (ions) per second in the sample after experiment minus the account in the initial sample. Using TIMS method, analyzed a Pd strip 1–2 mm thick and 20 mm in length, including a zone under the screen. The field volatilizes tens of angstrom unit from the sample surface during the analysis.

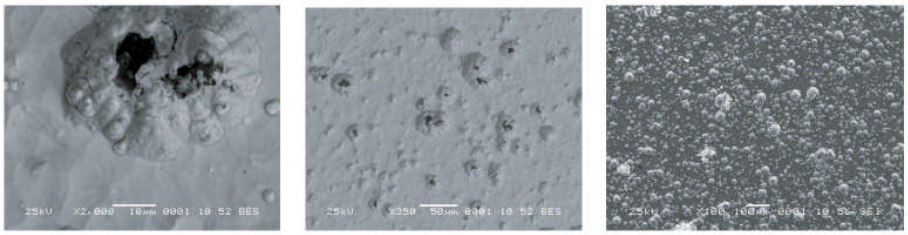

Fig. 1. Blisters on Pd surface after 22-hour deuterium discharge exposure. (a) Needle formations on the boundary of radiated and unirradiated areas. (b) Broken cocoon. (c) Microexplosion “crater”.

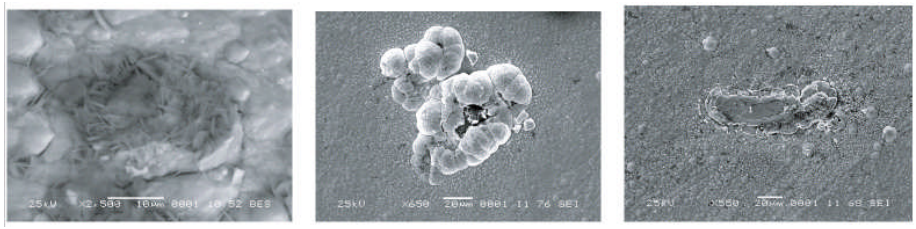

a. Needle formations on the boundary b. Broken cocoon. c. Micro explosion "crater"

Fig. 2. New formations on Pd surface after deuterium bombardment.

As can be seen in Table 13, the composition (in quantity and element content) of each element in the 1 μm-diameter point do not coincide (do not equal) with all analyzed Fig. 4a area 250 × 200 μm^2. The sample (1610/2) is one upper in eight foils-multilayer sample in this experiment. Upper sample was partly melted during experiment. However, heat balance was not estimated in this experiment.

The separate elements content, analyzed of 1610/2 area ~ 300 × 220 μm^2, with elements content on the 1 μm diameter area were compared. Data of Table 13 showed same difference in additional elements content and close values for main elements for homogeneous place of the surface.

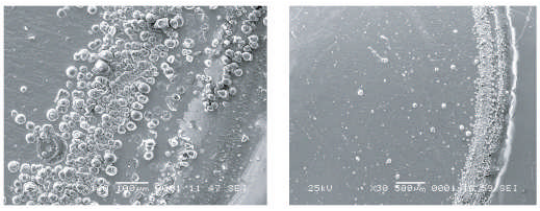

a. radiated and unirradiated areas b. radiated area on the left

Fig. 3. New formations on the boundary (a) of radiated and unirradiated areas (b) radiated area on the left Fig. 4c. The screened area from glow discharge radiation.

Table 12. Chemical composition change in new formations areas (Fig. 2c).

Element	Atomic percents					
	Point 1	Point 2	Point 3	Point 4	Point 5	Point 6
O		60.1 ± 1.2			21.5 ± 1.2	52.3 ± 1.5
Al	2.1 ± 0.9	0.5 ± 0.3				0.8 ± 0.2
Mg						1.5±0.5
Si			1.4±0.5			
Ti		4.3 ± 0.3				
Ga		0.5 ± 0.4	1.7 ± 0.6	1.6±0.9	1.5 ± 0.6	
Mo		1.6 ± 0.2	3.4 ± 0.6	4.2±0.8	2.6 ± 0.5	1.1 ± 0.3
Pd	97.9 ± 0.3	33.1 ± 0.7	93.5 ± 0.9	94.2±0.9	74.4 ± 1.1	40.7 ± 1.0

3.5. *Conformity Between Changes in Element Composition of Palladium and Structural Changes (Method EDX)*

The most essential changes of structure are observed with an increasing in discharge time. For example, numerous swellings - blisters (Fig. 1) and various growth

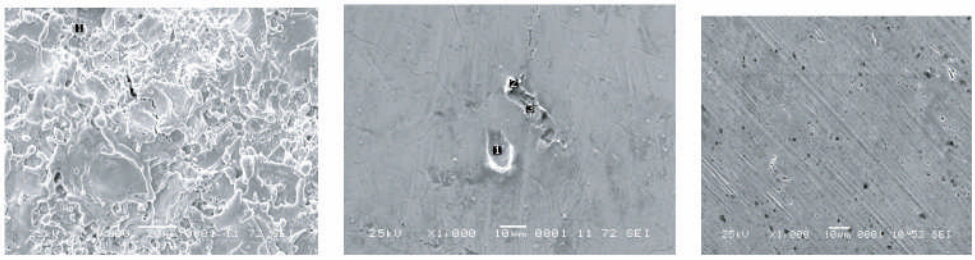

a. b. c.

Fig. 4. (a) Pd surface after deuterium irradiation by dose ~ 8×10^{21} sm^{-2}. (b) Screening zones (Pd # 1610, 30 mA, 400±20 V, P ~ 5Torr, 4 h in H→D. Set included eight foils. Three Pd foil were partially melted). Crater on the end of crack on back sample.

Table 13. Additional elements in Pd after deuterium bombardment (EDX, atomic percent).

Element	At. % , Fig. 4a (1610/1)		At. % , (1610/2)	
	Point 1 (1 μm)	All areas	Point1 (1μm)	All areas
O	13.3 ± 0.2	55.9 ± 1.2		
Na		1.2 ±0 .2		
Mg	1.4 ± 0.3	0.7 ± 0.1	1.25 ± 0.3	0.95 ± 0.3
Al	1.3 ± 0.2	0.9 ± 0.1	0.27 ± 0.3	0.53 ± 0.17
Si		0.4 ± 0.1	0.49 ± 0.2	0.25 ± 0.1
Ga	2.0 ± 0.2	0.8 ± 0.1	2.32 ± 0.25	2.32 ± 0.2
Mo	1.2 ± 0.1	0.82 ± 0.1	0.53 ± 0.16	0.47 ± 0.16
Pd	80.4 ± 0.4	39.13± 0.2	95.0 ± 0.3	95.36 ± 0.25
W	0.3± 0.05		0.12 ± 0.1	0.12 ± 0.08

formations are observed: needle-shaped growth and formations similar to cocoons (Figs. 2 and 3). Especially considerable changes of structure were observed on boundaries of the irradiated and unirradiated areas (Fig. 3). Examples of the structures forming after irradiation by low-energy ions and the element composition in these areas are explored in details (Figs. 3 and 4 and Tables 12 and 14).

4. Discussion. Transmutation Effect

Earlier it was shown that the irradiation by ions with energy <1 keV at glow discharge causes complexes of defects (dislocations and their aggregations, pores) depending on type of bombarding ions, temperature of irradiation and fluence of ions. The ions implantation with such energies can occur to depths of no more than several atomic layers. However, the radiation type defects under conditions of stress concentration gradient were formed.[14] In this case, the gas atoms are implanted to depths up to several millimeters. In addition, voids in volume of cathode material irradiated with low-energy ions are formed.[13] Earlier Matveenko (IAE "Kurchatov Center") showed (applied to the first wall of a thermonuclear reactor) that pressure in the pores under hydrogen ions energy of <1 keV could reach some hundreds of atmospheres.

The appearance of new elements absent in the sample and constructive parts of the apparatus before was found in the samples irradiated on glow-discharge cathode. An increase in the quantity of the impurity elements hundreds and thousands of times was revealed. Besides a change in the isotope ratio of elements from tens of percent up to hundreds of times[3] was observed. The analysis of the samples irradiated in glow discharge for more reliable results was carried out by several methods: a mass spectrometry and X-ray microanalysis in several Institutes of the country (including GIRedMet, IPhChAS, Tomsk Polytechnic Institute, "Lutch"). The greatest changes of the isotope and element composition were observed in "hot points": places of microexplosions, craters of plasma microdischarges.[9]

It is difficult to say what process is primary-microexplosions, microdischarges on structural inhomogeneities, growth formations, and phase inserts; or formation of new elements and phase segregations in places of microexplosions is the result of elements transmutations in the micromelting zones. New elements formation as the result of DD-reactions at the cracks edges with oxide films, so-called accelerating effect, is possible too. It might be the consequence of "overvoltages" incipient on "spikes" formations (cone-shaped or needle-shaped) and resulting in instantaneous micromeltings or microexplosions. In these cases, processes similar to the processes in constructional materials of the nuclear reactors with the formation of micromeltings zones ("thermal" peaks) are possible, too. It is difficult to estimate the priority of these processes. Every possible, the ions concentration gradient and temperature gradient can contribute to the change of cathode structure. Ivanov[11] showed that a formation of pulsing microplasma discharges (unipolar arcs) on structural irregularities (heterogeneities), impurities segregation and oxide films in the surface material layer was possible.

Examination of the radioactivity change, the isotope and element composition of the uranium samples (uranium component decrease and thorium component increase by gamma-spectrometry, mass spectrometry and EDX) in glow discharge showed the opportunity of stimulation of nuclear transmutations processes under low-energy actions.[7,8] It is impossible to explain the increase of integrated αt, βt, γt uranium emission and the change of ratio of uranium energy peaks and its daughter elements (^{231,234}Th and ^{234}U) after experiments in glow discharge by pollution (impurity) from medium (environment) or by some other effects.

The maximum quantity of additional elements at glow discharge experiments should be observed under equivalent conditions for heavier ions (e.g., an argon) if "additional" elements appearance is a result of cathode sputtering or redistributions of these elements in volume of the ion irradiated material. These quantities should grow according to masses and ionic radiuses of bombarding ions in the following sequence: a minimum quantity for the hydrogen irradiated samples, a greater quantity—for deuterium irradiated samples, and a maximum quantity for heavy-ions irradiated samples (argon and xenon), respectively. We observed a maximum quantity of additional elements and their maximum variety at deuterium discharges. Smaller quantities of these elements and a smaller variety of them were observed at hydrogen discharges and minimum of variety for argon and xenon.[2] One can see that the peak effect on characteristic spectrums was for experiments in deuterium. Dependence of additional elements quantity on ions current density and on temperature of process is very significant and ambiguous. In this case, it is difficult to take into account the action of plurality of simultaneously proceeding processes. Probably, both new additional elements formation and preferable sputtering of lighter elements simultaneously occur under low-energy ions irradiation. The accelerated (speeded) surface diffusion, the impurity components segregations near dislocations and other defects are also take place. A series of experiments[4] showed a dependence of the element composition change on current density and working gas composition (medium) (Tables 6 and 7). So, a maximal increase of Ag quantity was observed for the greatest current density of 35 mA/sm^2 (250 times or from 20 up to 5000 ppm). A comparison of the discharge in hydrogen, deuterium and the discharge with preliminary irradiation in hydrogen and then in deuterium showed, that additional quantity of Ag appearance was minimal (up to 200 ppm). The isotope and element composition changes essentially depend on such parameter of process as current sort. The isotope changes obtained by TIMS method for experiments with direct current are given in Tables 7 and 8 and with pulsing current in Tables 9 and 10. A significant change was observed for $^{56/57}$Fe ($\sim$1000) in pulsing current experiment, this change being significant not only on value of ratio, but also on absolute value. So, for a sample after experiment with pulsing current $N(N^{57}\text{Fe}–N^{56}\text{Fe}) = 3840$ cps, and the natural iron 56/57 isotopes ratio is about 40, 56/57 isotope ratio after experiment is $\sim$0.04. The 56/57 isotopes ratio for Sample 1610 at direct current was $\sim$10. It means that the ratio decreases 4 times due to an increase of the contribution of ^{57}Fe (a heavier isotope). Thus, a change in

the $^{56/57}$Fe isotope ratio by a factor of more than 100 for experiment with pulsing current was observed.

For the same Sample 1610 the isotope ratio of $^{48/47}$Ti increases ∼2.5 times and $^{48/46}$Ti increases almost ∼3.8 times due to a decrease of contribution of a heavier isotope (the most spread ^{48}Ti isotope). The $^{52/53}$Cr isotope ratio also decreases due to a decrease of contribution of heavier isotope 53. Thus, it is impossible to explain this effect by sputtering of a lighter isotope or by isotopes separation. Also it is impossible to explain it by diffusion coefficient.

The $^{56/57}$Fe isotope ratio in 1694 as compared with natural ratio of isotopes is ∼2.3 (Table 1). The $^{48/46}$Ti isotope ratio comparison is about ∼5.46. Samples No. 1610 and No. 1694 had different experimental conditions. So No. 1610 was a multilayered compound and after experiment some melting areas and even cracks were found on it and No. 1694 was single-layered and its surface after experiment was more homogeneous.

We would like to pay special attention to detection of isotopes with mass number 59 (Co), cps of which was $\sim 10^3$ cps, for 55 (Mn) $\sim 10^3$ cps, for 45 (Sc) $\sim 10^2$ cps. They were found in a plenty in the samples after experiment but they were found in initial samples.

The comparison of the quantity of the elements analyzed by method SMS with possible reactions of fusion-fission of nucleus is given in Table 15 in view of conformity of their masses, their spin and parity. The opportunity of simultaneous appearance of particular isotopes groups in samples is supposed, i.e. formation of such elements as Mg and Br (1); Mg and As (2); Si and As (3) in the same low-energy process in glow discharge.

The variants of the reactions given in the table are possible from the results of the analysis. It is possible to see the presence of isotopes with mass numbers 26 and 80 as results of reactions (1–4), 19 and 88 - reaction (5), 50 and 56 - reaction (6) in one analyzed sample.

It could be possible to explain the appearance of chemical elements in the samples irradiated by ions in glow discharge by such reactions, but the high Coulomb barrier makes the probability of such processes insignificant. Rodionov[12] paid attention to the fact that the Coulomb barrier is a classical concept and the representation of it at nuclear distances does not work. It means that the concept of the Coulomb barrier is not meaningful in quantum ensembles for low energies of interacting particles. It makes possible multinuclear reactions in low-energy processes.

Therefore, it is supposed that Fe, Ni, and Ti can appear in the following reactions:

$$\alpha + {}^{102}_{46}\mathrm{Pd} \rightarrow {}^{46}_{22}\mathrm{Ti} + {}^{60}_{26}\mathrm{Fe}^{*} + 20.1\,\mathrm{MeV}, \tag{7}$$

$$\text{or} \rightarrow {}^{48}_{22}\mathrm{Ti} + {}^{58}_{26}\mathrm{Fe} + 25.1\,\mathrm{MeV}, \tag{8}$$

$$\text{or} \rightarrow {}^{50}_{22}\mathrm{Ti} + {}^{56}_{26}\mathrm{Fe} + 26.5\,\mathrm{MeV}. \tag{9}$$

Table 14. Additional elements in structure formations after deuterium experiments (atomic %, EDX)*

Element	Boundary 1	2	3	"Flower" Fig. 4a		Screened zone	Point 1	Point 2	Point 3	All zones	Point 4	Point 5	Point 6
1	2	3	4	5	6	7	8	9	10	11	12	13	14
O	73.3±0.7	69.3±0.7	43.4±1.2		16.4±1.5	4.3±1.3		26.4±0.2		22.4±2.1	38.3±1.3	66.2±0.7	
Na	0.13±0.05	0.13±0.10						1.7±0.4		3.1±0.3	0.63±0.25		
Mg	0.12±0.04	0.2±0.1	1.0± 0.2	1.2±0.3	1.1±0.2	0.9±0.3	1.6±0.3	0.8±0.2	1.6±0.1	0.96±0.2	0.75±0.19	0.30±0.06	1.54±0.3
Al	2.05±0.04	1.8±0.1	3.4±0.2					2.2±0.1		0.5±0.13	3.8±0.1	10.8±0.1	
Si	0.3±0.1	0.3±0.1	1.0±0.1		0.4±0.1			0.6±0.1	0.5±0.1	0.3±0.15	0.27±0.1		
K								0.8±0.1					
S			4.1±0.2										
Fe	0.06±0.03								0.2±0.1	0.20±0.07	0.12±0.06		
Ni									0.2±0.1				
Ga	0.22±0.05	0.4±0.1	0.8±0.2	2.2±0.2	1.6 ± 0.1	1.6±0.2	2.3±0.2	1.1±0.2	2.0±0.2	1.5±0.2	1.35±0.13	0.37±0.05	2.1±0.2
Sr	0.06±0.03		0.2±0.1										
Mo	9.4±0.1	8.0±0.1			0.6±0.1		0.4±0.1				0.16±0.08	0.10±0.04	
Pd	13.6±0.1	19.2±0.1	44.5±0.3	92.6±0.7	74.1±1.1	92.3±0.4	95.0±0.3	66.3±0.3	95.0±0.3	70.8±0.3	54.5±0.3	22.1±0.1	95.9±0.3
Cd	0.17±0.5	0.14±0.05	0.2±0.1	0.4± 0.1									
Ac	0.35±0.05	0.5±0.06	1.2±0.1	2.8±0.3	2.9±0.25								
Pb	0.14±0.04	0.2±0.05				0.2±0.06	0.2±0.1		0.17±0.08		0.16±0.08	0.04±0.02	
Sn					0.54±0.1	0.15±0.1							
W						0.6±0.1	0.6±0.1	0.21±0.07		0.16±0.06		0.08±0.04	0.07±0.02

*Voltage 25 kV, # 1694.

However, for reactions (7–9) with the participation of α-particles, first the following possible reactions are to proceed:

$$\mathrm{d} + {}^{104}_{46}\mathrm{Pd} \to {}^{22}_{10}\mathrm{Ne} + {}^{80}_{35}\mathrm{Br}^* + \alpha + 5.21\,\mathrm{MeV}, \tag{10}$$

$$\mathrm{d} + {}^{105}_{46}\mathrm{Pd} \to {}^{23}_{10}\mathrm{Ne}^* + {}^{80}_{35}\mathrm{Br}^* + \alpha + 3.3\,\mathrm{MeV}, \tag{11}$$

$$\mathrm{d} + {}^{108}_{46}\mathrm{Pd} \to {}^{4}_{8}\mathrm{Be}^* + {}^{98}_{41}\mathrm{Nb}^* + \alpha + 2.75\,\mathrm{MeV}, \tag{12}$$

$$^{98}_{41}\mathrm{Nb}^* \to 51\mathrm{M}{:}\beta^- 2.3, 1.9 : \gamma 787.3, 722.7 \to {}^{98}_{42}\mathrm{Mo},$$

Table 15. Isotopes ratio in possible nuclear reactions in Sample No. 1734 (SMS).

Mass	cps	Possible reactions	
26	40	$\mathrm{d} + {}^{104}_{46}\mathrm{Pd} \to 12{}^{26}\mathrm{Mg} + {}^{80}_{35}\mathrm{Br}^* + 15.8$;	1
		${}^{80}_{35}\mathrm{Br}^* \to 17.66\mathrm{M}{:}\beta^- 2.00 : \gamma 616.6 \to {}^{80}_{36}\,\mathrm{Kr}$;	
		or ${}^{80}_{35}\mathrm{Br}^* \to 17.66\mathrm{MeV} : \beta^+ .85 : \times\gamma 616.6 \to {}^{80}_{34}\mathrm{Se}$	
		$\mathrm{d} + {}^{108}_{46}\mathrm{Pd} \to {}^{26}_{12}\mathrm{Mg} + {}^{80}_{33}\mathrm{As}^* + \alpha + 12.2$;	2
80	60000	${}^{80}_{33}\mathrm{As}^* \to 16\mathrm{S}{:}\beta^- 5.4, 4.7 : \gamma 665.9 \to {}^{80}_{34}\mathrm{Se}$	
		$\mathrm{d} + {}^{104}_{46}\mathrm{Pd} \to {}^{26}_{14}\mathrm{Si}^* + {}^{80}_{33}\mathrm{As}^* + 2.63\,\mathrm{MeV}$	3
		$\alpha + {}^{102}_{46}\mathrm{Pd} \to {}^{26}_{12}\mathrm{Mg} + {}^{80}_{36}\mathrm{Kr} + 8.60\,\mathrm{MeV}$	4
		${}^{26}_{14}\mathrm{Si}^* \to 2.235\mathrm{S}{:}\beta + 3.83 : \gamma 829 \to {}^{26}_{13}\mathrm{Al}^* \to 6.345\mathrm{S}{:}\beta + 3.21 \to {}^{26}_{12}\mathrm{Mg}$	
		${}^{26}_{13}\mathrm{Al}^* \to 7.3\mathrm{E}5\ \mathrm{A}{:}\beta + 1.17 : \gamma 1808.6 \to {}^{26}_{12}\mathrm{Mg}$	
19	80	$\mathrm{p} + {}^{106}_{46}\mathrm{Pd} \to {}^{19}_{9}\mathrm{F} + {}^{88}_{38}\mathrm{Sr} + 4.42\,\mathrm{MeV}$	5
88	50		
50	30	$\alpha + {}^{102}_{46}\mathrm{Pd} \to {}^{50}_{22}\mathrm{Ti} + {}^{56}_{26}\mathrm{Fe} + 26.5\,\mathrm{MeV}$	6
56	18		

$$\mathrm{d} + {}^{104}_{46}\mathrm{Pd} \to {}^{30}_{15}\mathrm{P}^* + {}^{72}_{30}\mathrm{Zn}^* + \alpha + 9.64\,\mathrm{MeV},$$

$$\alpha + {}^{102}_{46}\mathrm{Pd} \to {}^{22}_{10}\mathrm{Ne} + {}^{84}_{38}\mathrm{Sr} + 3.16\,\mathrm{MeV},$$

$$\alpha + {}^{102}_{46}\mathrm{Pd} \to {}^{18}_{10}\mathrm{Ne}^* + {}^{88}_{38}\mathrm{Sr} + 2.92\,\mathrm{MeV},$$

$$\alpha + {}^{104}_{46}\mathrm{Pd} \to {}^{22}_{10}\,\mathrm{Ne} + {}^{86}_{38}\mathrm{Sr} + 5.55\,\mathrm{MeV},$$

$$\alpha + {}^{106}_{46}\mathrm{Pd} \to {}^{24}_{10}\mathrm{Ne}^* + {}^{86}_{38}\mathrm{Sr} + 2.98\,\mathrm{MeV},$$

$$\alpha + {}^{108}_{46}\mathrm{Pd} \to {}^{22}_{10}\mathrm{Ne} + {}^{90}_{38}\mathrm{Sr} + 6.85\,\mathrm{MeV}$$

It is necessary to note that TIMS in analyzed samples revealed masses of isotopes 18 and 22 to a small extent many times. Isotopes of molybdenum were always present significantly. As it was noticed earlier, molybdenum could also be a consequence of its over-sputtering from the surface of the sample holder. Mass of isotope

22 in a quantity of 60 cps and mass 80 in a quantity of 95 cps were also observed in this spectrum.

$$\mathrm{d} + {}^{102}_{46}\mathrm{Pd} \rightarrow {}^{22}_{10}\mathrm{Ne} + {}^{82}_{37}\mathrm{Rb} + 5.90\,\mathrm{MeV}.$$

Masses 22 and 82 were also present in TIMS spectrums of this sample in quantities of 60 and 540 count per second (cps). It is necessary to note that the instable finding of Ag by method EDX[6] could be a result of formation

$${}^{108}_{47}\mathrm{Ag}^{*}_{,}\ {}^{106}_{47}\mathrm{Ag}^{*}_{,}\ {}^{108}_{47}\mathrm{Ag}^{*}_{,}\ {}^{110}_{47}\mathrm{Ag}^{*}$$

in the following reactions with the further transmutation of these isotopes into stable.

$$\mathrm{d} + {}^{104}_{46}\mathrm{Pd} \rightarrow {}^{106}_{47}\mathrm{Ag}^{*} + 10.7\,\mathrm{MeV},$$

$${}^{106}_{47}\mathrm{Ag}^{*} \rightarrow \underline{24.0M : \beta^{-}}\,\underline{1.96 : \gamma 511.9} \rightarrow {}^{106}_{48}\mathrm{Cd},$$

$$\mathrm{d} + {}^{106}_{46}\mathrm{Pd} \rightarrow {}^{108}_{47}\mathrm{Ag}^{*} + 10.8\,\mathrm{MeV},$$

$${}^{108}_{47}\mathrm{Ag}^{*} \rightarrow \underline{2.39M : \varepsilon : \beta^{-}}\,\underline{1.65 : \gamma 633.0} \rightarrow {}^{108}_{48}\mathrm{Cd}$$

$$\mathrm{d} + {}^{108}_{46}\mathrm{Pd} \rightarrow {}^{110}_{47}\mathrm{Ag}^{*} + 11.1\,\mathrm{MeV},$$

$${}^{110}_{47}\mathrm{Ag}^{*} \rightarrow \underline{24.6S : \beta^{-}}\,\underline{2.981 : \gamma 657.8} \rightarrow {}^{110}_{48}\mathrm{Cd}.$$

The opportunity of going above described reactions with the formation of argentums isotopes in an excited state and their subsequent transition into stable state can help to understand that the results of finding many elements change with a change in the interval of the samples analysis time after the experiment termination. This fact is undoubtedly important, and it is necessary to take into account when isotopes quantity and their composition are to be correctly estimated, as the performance of the analysis at the time planned after the experiment termination is not always feasible.

5. Conclusion

1. The complex of examinations showed that changes of structure and element composition in the samples irradiated by glow discharge ions depended on: (a) density of ions flow, (b) dose of irradiating ions, (c) kind of irradiating ions, and (d) sort of current and other parameters of process.
2. Dependence on parameters is ambiguous as some factors simultaneously affect the change of composition.
3. More homogeneous structure and more homogeneous change of composition are observed for long experiments.

4. Maximum changes of element composition are observed in " hot (active) points " - micro craters, areas of micromelting and others new structural formations.
5. Various methods of low-energy action on different materials give a formation of plurality of basic elements (Si, Al, Mg, and Ca) found by various methods of the analysis of these materials. Such more rare elements as Mn, Sc, Co, Sr, Ne, and Ba were found in a smaller extent.
6. The peak changes of the 56/57 iron isotope composition (1000 times) were observed for pulsed current.
7. A comparison of elements and isotopes found by various analysis methods with possible types of fusion-fission reactions is carried out.

Acknowledgements.

Authors express the gratitude to corresponding member of the Academy of Sciences I.I. Fedik ("Lutch") and Professor, Dr. B.U. Rodionov (MEPhI) for valuable notes by preparation of this article.

References

1. I. Savvatimova, Ya. Kucherov, and A. Karabut, *Transaction of Fusion Technology* **26**, 4T, 389 (1994).
2. I. Savvatimova, A. Senchukov, and I. Chernov , *ICCF6*, Progress in new hydrogen energy. Japan (1996), p. 575.
3. I. Savvatimova, A. Karabut, Nuclear Reaction Products Registration. Surface, Moscow: RAN (1996), Vol. 1, p. 63.
4. I. Savvatimova B, Karabut A.B., Radioactivity of the Pd cathode after GD. Surface, Moscow: RAN (1996), Vol. 1, p. 76.
5. I. Savvatimova, Transmutation in cathode materials at GD. *ICCF-7*, Canada (1998), p. 342.
6. I. Savvatimova, Reproducibility of experiments in GD, *ICCF8*, Italian Phys. Society, Italy (2000), p. 277.
7. J. Dash, I. Savvatimova and H. Kozima, Effects of GD on Radioactivity *Proc. ICENES 2002* (2002), p. 122
8. J. Dash, and I. Savvatimova, Effects of glow discharge with hydrogen isotope plasmas on radioactivity of uranium, *Proc. ICCF10*, Bejing, China, 2002.
9. I. Savvatimova and D. Gavritenkov, Results of Ti analysis after GD. *Proc. ICCF11* (2004).
10. A. Karabut, Ya. Kucherov, and I. Savvatimova, Possible nuclear reactions mechanisms at glow discharge in dseuterium. *Proc. ICCF3*, Japan (1992), p. 165
11. V. Ivanov, Excitation and effect of microplasma discharges on metals and alloys in a microwave plasma torch, *Applied Physics* **B2**, 5(2001).
12. Rodionov, *Proc. 12* Rus. CF Conf. 2004, Moscow (2005), p. 110.
13. Ya. Kucherov, A. Karabut, and I. Savvatimova, *Phys. Let.* **A170**, 265 (1992).
14. G. Vorontzova, and I. Savvatimova, *Atomic Energy* **69**(5), 297 (1990).